Received Date: 16-Apr-2014

Accepted Date: 23-Dec-2014

Article Type : Primary Research Articles

Leaf and stem economics spectra drive diversity of functional plant traits in a dynamic global vegetation model

Running title: Diversifying plant traits in a DGVM

B. Sakschewski[1,2], W. von Bloh[1,2], A. Boit[1,2], A. Rammig[1,2], J. Kattge[3], L. Poorter[4], J. Peñuelas[5,6], K. Thonicke[1,2]

[1]Potsdam Institute for Climate Impact Research (PIK), Telegraphenberg A31, 14473 Potsdam, Germany

[2]Berlin-Brandenburg Institute of Advanced Biodiversity Research (BBIB), 14195 Berlin, Germany

[3]Max-Planck-Institute for Biogeochemistry, 07745 Jena, Germany

[4]Forest Ecology and Forest Management Group, Wageningen University, PO Box 47, 6700AA Wageningen, Netherlands

[5]CSIC, Global Ecology Unit CREAF-CSIC-UAB, Cerdanyola del Vallés 08193, Catalonia, Spain

This article has been accepted for publication and undergone full peer review but has not been through the copyediting, typesetting, pagination and proofreading process, which may lead to differences between this version and the Version of Record. Please cite this article as doi: 10.1111/gcb.12870

[6]CREAF, Cerdanyola del Vallès 08193, Catalonia, Spain

Corresponding authors information: Telephone: +49 331 288 2458; Fax +49 331 288 2620; boris.sakschewski@pik-potsdam.de

Keywords: dynamic global vegetation model, functional diversity, trait variability, trade-off, leaf economics spectrum, individual-based model, gap model, Amazon rainforest

Paper type: Primary research article

Abstract

Functional diversity is critical for ecosystem dynamics, stability and productivity. However, dynamic global vegetation models (DGVMs) which are increasingly used to simulate ecosystem functions under global change, condense functional diversity to Plant Functional Types (PFTs) with constant parameters. Here, we develop an individual- and trait-based version of the dynamic global vegetation model (DGVM) LPJmL (**L**und-**P**otsdam-**J**ena **m**anaged **L**and) called LPJmL-FIT (LPJmL with **F**lexible **I**ndividual **T**raits) which we apply to generate plant trait maps for the Amazon basin. LPJmL-FIT incorporates empirical ranges of five traits of tropical trees extracted from the TRY global plant trait database, namely specific leaf area (*SLA*), leaf longevity (*LL*), leaf nitrogen content (N_{area}), the maximum carboxylation rate of RUBISCO per leaf area ($Vcmax_{area}$), and wood density (*WD*). To scale the individual growth performance of trees, the leaf traits are linked by trade-offs based on the leaf economics spectrum, whereas wood density is linked to tree mortality. No pre-selection of growth strategies is taking place, because individuals with unique trait combinations are uniformly distributed at tree establishment. We

validate the modeled trait distributions by empirical trait data and the modeled biomass by a remote sensing product along a climatic gradient. Including trait variability and trade-offs successfully predicts natural trait distributions and achieves a more realistic representation of functional diversity at the local to regional scale. As sites of high climatic variability, the fringes of the Amazon promote trait divergence and the coexistence of multiple tree growth strategies, whilst lower plant trait diversity is found in the species-rich center of the region with relatively low climatic variability. LPJmL-FIT enables to test hypotheses on the effects of functional biodiversity on ecosystem functioning and to apply the DGVM to current challenges in ecosystem management from local to global scales, i.e. deforestation and climate change effects.

Introduction

The links between biodiversity effects and ecosystem functioning (hereafter BEF) (2012; Hooper *et al.,* 2012; Naeem *et al.,* 1994) are still insufficiently understood and are therefore in the spotlight of ecological research (Hooper *et al.,* 2005; Loreau *et al.,* 2001; Naeem & Wright, 2003; Balvanera *et al.,* 2006). In particular, functional diversity supports ecosystem functioning (Sterk *et al.,* 2013; Suding *et al.,* 2008; Violle *et al.,* 2007), stability and productivity (McCann, 2000; Morin *et al.,* 2011; Diaz & Cabido, 2001), and resilience against disturbances and environmental variability (Mori *et al.,* 2013).

To predict ecosystem functioning at regional to global scales (Sitch *et al.,* 2008), dynamic global vegetation models (DGVMs) (Prentice *et al.,* 1992) simulate processes of vegetation dynamics and hydrology. However, most current DGVMs condense functional diversity to the smallest scale possible by using Plant Functional Types (PFT) (Woodward & Kelly, 1997) in a monoculture-like approach at the biome level (Poulter *et al.,* 2011; Scheiter *et al.,* 2013) with fixed bioclimatic limits and often calibrated parameters which prescribe their simulated performance under varying environmental conditions. This reductionist PFT approach eliminates sources of natural trait variability which, at the time of model design, was inevitable due to the lack of plant trait data and computational power.

With increased computational capabilities, the preconditions to better acknowledge natural functional diversity and plant trade-offs in DGVMs are generally fulfilled (Van Bodegom *et al.,* 2012). At the same time, there is a recent boost in trait-based ecology that aims to identify leading axes of plant strategy variation (Westoby & Wright, 2006), and a growing theoretical and empirical body on global plant trait spectra related to the economics of leaves and stems (Baraloto *et al.,* 2010; Chave *et al.,* 2009; Kattge *et al.,* 2011; Wright *et al.,* 2004). Bridging the gap between the research fields of DGVMs and functional ecology by modelling trait variability is crucial to disentangle the influence of abiotic factors from BEF in a spatio-temporally heterogeneous environment (Hector & Bagchi, 2007; Hillebrand & Matthiessen, 2009; Reiss *et al.,* 2009). Such an approach would also take the empirical trait-based approach important steps further by 1) scaling up from individual tissue traits to whole-plant performance, ecosystem processes and services, and 2) providing a better predictive framework for ecological patterns and their societal consequences at larger spatial and temporal scales (Van Bodegom *et al.,* 2012).

We re-implemented the existing DGVM LPJmL (**L**und-**P**otsdam-**J**ena **m**anaged **L**ands) (Bondeau *et al.,* 2007; Sitch *et al.,* 2003) with **f**lexible **i**ndividual **t**raits (LPJmL-FIT) as an individual-based gap model (Bugmann, 2001; Taylor *et al.,* 2009). This allows simulating individual trees with unique trait combinations which compete for resources within a distinctive patch. We applied LPJmL-FIT to generate plant trait maps for the Amazon region because the Amazon is the largest remaining forest with high tree functional diversity on Earth (Kraft *et al.,*

2008) and of critical importance for the global carbon cycle and carbon-cycle-climate feedbacks (Cox *et al.,* 2013). This is the first study, where detailed, basin-wide patterns in trait distributions and diversity of functional plant traits are quantified applying a trait-based DGVM. We conducted a series of simulation experiments to assess the effects of model complexity on the resulting trait distributions, diversity of plant traits, and vegetation carbon.

LPJmL-FIT features 5 variable plant traits connected via trade-offs derived from global plant trait data. This opens up a realistic global trait space. We focus on the traits specific leaf area (*SLA*), leaf longevity (*LL*), leaf nitrogen content (N_{area}), the maximum carboxylation rate of RUBISCO per leaf area ($Vcmax_{area}$) and wood density (*WD*) because these traits determine the individual performance of tree individuals through their effects on growth and mortality (Violle *et al.,* 2007). The leaf traits are linked by empirically established trade-offs based on the leaf economics spectrum (LES) (Reich *et al.,* 1997; Reich *et al.,* 1999; Shipley *et al.,* 2006; Wright *et al.,* 2004) which describes a set of leaf trade-offs explaining worldwide leaf investment strategies. *WD* is linked to tree mortality following the idea of the stem economics spectrum (SES, Baraloto *et al.,* 2010).

The main objective of this study is to develop a generalizable approach which incorporates continuous plant traits and their respective trade-offs in DGVMs 1.) to add ecological realism to DGVMs by improving their representation of functional diversity by plant trait distributions, and 2.) to predict observed plant trait distributions and biomass. This way, we lay the foundations to test BEF related hypotheses, e.g. the insurance hypothesis, by associating changes in trait means, ranges and trade-offs with their effect on functional diversity and ecosystem-level indicators of plant performance, e.g. biomass. Principally globally applicable, such a DGVM may complement the existing empirical knowledge of functional diversity and its relation to ecosystem functions.

Few other vegetation models such as the JEDI-DGVM (Pavlick *et al.,* 2012; Reu *et al.,* 2011a; Reu *et al.,* 2011b), the aDGVM2 (Scheiter *et al.,* 2013), the trait-based version of the JSBACH model (Verheijen *et al.,* 2013), and most recently, the Traits-based Forest Simulator (TFS) (Fyllas *et al.,* 2014) also build upon trait-based growth strategies. Our DGVM approach differs from those models or their specific components for several reasons: LPJmL-FIT establishes individual trees with a number of variable traits. These traits range within their globally observed boundaries in natural ecosystems because their ranges are constrained by empirically-derived trade-offs following the theory of LES and SES. This opens a multi-dimensional trait space including all ecologically reasonable trait combinations. Each of these trait combinations has the same probability to be assigned at tree establishment because no pre-selection (e.g. due to bioclimatic limits) is applied. During simulated vegetation dynamics, all possible trait combinations compete for light and water within the study area. The trait combinations which are best adapted to local environmental conditions survive and represent a subset of the initialized trait space which is then validated against observed trait data.

We discuss the relevance of our findings for ecosystem theory and its applications, i.e. up-scaling effects of continuous traits to whole plant-performance and their influence on trait distributions at the regional scale, thereby accounting for spatio-temporal heterogeneity, and conclude with an outlook on future DGVM applications in the prediction of future ecosystem transitions under global change such as the uncertain future of the Amazon rainforests (Cox *et al.,* 2000; Cox *et al.,* 2013; Rammig *et al.,* 2010; Malhi *et al.,* 2009).

Materials and methods

LPJmL-FIT: a new gap model version of LPJmL with Flexible Individual Traits

Standard LPJmL is a process-based dynamic global vegetation model (DGVM) with 9 generic plant functional types (PFTs) representing natural vegetation at the level of biomes (Gerten *et al.,* 2004; Schaphoff *et al.,* 2013; Sitch *et al.,* 2003), 12 crop functional types (CFTs) and managed grass (Bondeau *et al.,* 2007). We re-implemented LPJmL in a gap model approach to account for the competitive effects between tree individuals with unique key trait combinations forming a highly diverse community of possible tree growth strategies. We deliberately model tree individuals with unique trait combinations, but not species, to elucidate how selective processes (i.e. environmental filtering and local competition) influence the performance of tree growth strategies. This level of abstraction allows to investigate how functional diversity influences community assembly, functional composition and ecosystem functioning in a computationally feasible and spatially scalable approach.

To provide an overview about the structure of the new LPJmL-FIT model (cf. Fig. 1), we first discuss tree establishment (Section 1.1), vegetation dynamics (1.2) and model output (1.3), and then shortly describe the modelling protocol (1.4) and validation procedures (1.5). All data processing and statistical analysis described in the methods sections was done with the commercial software MATLAB® (MATLAB and Statistics Toolbox Release 2012b).

1.1 Tree establishment

Selection of key plant traits to be diversified in LPJmL-FIT

All empirical plant trait data were obtained from the global plant trait database TRY (Kattge *et al.*, 2011) and were filtered for worldwide broadleaved tree entries to investigate worldwide tree trait interrelations. We used worldwide data to create a generalizable approach enabling to make worldwide simulations. Rather than using averaged species trait values, we used all observations of broadleaved trees recorded in the TRY data base to conserve the intraspecific variability of traits. We focused on 5 key traits that are thought to capture the major axes of strategy variation across land plants, as they are related to the leaf economics spectrum (LES, Wright *et al.* 2004) and the stem economics spectrum (SES, Baraloto *et al.,* 2010). Traits included are specific leaf area (*SLA, leaf area per unit leaf mass,* mm^2 mg^{-1}), leaf longevity (*LL, average lifespan of leaves, in months*), leaf nitrogen content per leaf area (N_{area}, mg g^{-1}), maximum carboxylation rate of RUBISCO enzyme per leaf area ($Vcmax_{area}$, µmol CO_2 m^{-2} s^{-1}) and wood density (*WD, wood dry mass per unit of green volume*, g cm^{-3}). All TRY data we used relates to the following original references: (Atkin *et al.,* 1999; Campbell *et al.,* 2007; Castro-Diez *et al.,* 1998; Chave *et al.,* 2009; Cornelissen *et al.,* 1996; Cornelissen, 1996; Cornelissen *et al.,* 2003; Cornelissen *et al.,* 2004; Cornwell *et al.,* 2008; Diaz *et al.,* 2004; Fonseca *et al.,* 2000; Freschet *et al.,* 2010; Fyllas *et al.,* 2009; Garnier *et al.,* 2007; Gutierrez & Huth, 2012; Kattge *et al.,* 2009; Kleyer *et al.,* 2008; Kurokawa & Nakashizuka, 2008; Laughlin *et al.,* 2010; Loveys *et al.,* 2003; Medlyn *et al.,* 1999; Messier *et al.,* 2010; Niinemets, 2001; Ogaya & Penuelas, 2003; Ordonez *et al.,* 2010; Penuelas *et al.,* 2010; Poorter *et al.,* 2009; Preston *et al.,* 2006; Quested *et al.,* 2003; Reich *et al.,* 2008; Reich *et al.,* 2009; Shiodera *et al.,* 2008; Shipley & Vu, 2002; Shipley, 2002; Swaine, 2007; Willis *et al.,* 2010; Wright *et al.,* 2004; Wright *et al.,* 2007; Wright *et al.,* 2010; Xu &

Baldocchi, 2003).

Implementing trade-offs and diversifying model parameters

LPJmL-FIT implements three trade-offs (a-c), two of which (a-b) are part of the LES (Wright *et al.,* 2004). The third trade-off (c) is part of the SES and accounts for the empirically observed negative relationship between wood density and tree mortality (see e.g. Chave *et al.,* 2009 and references below). Detailed information on all derived regression functions, underlying composition and geographical origin of data is given in Data S1 (Eq. 1-3; Fig. S1-S4).

a.) The *SLA-LL* trade-off and its relation to N_{area} and tree phenology

There is a spectrum in leaf traits, running from productive short-lived leaves with high carbon returns and nutrient investments, to conservative, long-lived leaves with slow returns on investments. This implies a trade-off between potential rates of carbon return and the respective duration of return along the *SLA-LL* spectrum (Kikuzawa, 1995; Reich *et al.,* 1997; Westoby *et al.,* 2000; Westoby *et al.,* 2002). Thin and/or soft leaves (i.e. with a high *SLA*) generally require little carbon investment per unit leaf area and are physiologically more active. In contrast, leaves with low *SLAs* have higher *LLs*, because they invest more carbon per unit leaf area in defense structures making them more durable against physical stress and herbivory. This general pattern also holds for trees in the Amazon region (Poorter & Bongers, 2006; Reich *et al.,* 1991; Reich *et al.,* 2004), and scales up to a growth–survival trade-off at the whole-plant level (Kikuzawa & Lechowicz, 2011; Poorter & Bongers, 2006; Poorter *et al.,* 2008; Ruger *et al.,* 2012; Sterck *et al.,* 2006).

In seasonal environments, periodical unfavorable conditions, e.g. drought or cold, force trees to shed their leaves, thereby setting an upper limit to *LL*. A high *SLA* is advantageous in such a seasonal environment, as it optimizes carbon gain during the short growing season. However, a low *LL* is not only the result of climatic forcing, but also occurs due to the often higher palatability of high *SLA* leaves which tend to have high nutrient concentrations per unit leaf mass (Poorter & Evans, 1998) and smaller investments in leaf defenses (Kitajima & Poorter, 2010).

A low *SLA* is usually the response to stable climatic conditions and shaded conditions as in tropical rainforests. Here, a low *SLA* can bear an advantage, because the nutrient-poor soils and low light environment of tropical rainforests favor leaves which store nutrients and carbon for a longer time period. A high *LL* increases the residence time of nutrients and carbon in the plant and therefore enhances the photosynthetic revenue stream of carbon and nutrient investment in leaves (Kikuzawa & Lechowicz, 2011).

In standard LPJmL, *LL* is a fixed empirical parameter for each PFT from which the PFT's *SLA* value is derived. In LPJmL-FIT, in contrast, we infer *LLs* from the empirical *SLA* range in the TRY database via regression functions (Data S1) to account for the continuum of *LL*s observed in nature (Chabot & Hicks, 1982; Kikuzawa & Lechowicz, 2011; van Ommen Kloeke *et al.,* 2012).

Standard LPJmL describes two phenology types in the tropics, "evergreen" and "deciduous". A fixed *LL* for evergreen and deciduous trees is accompanied by a PFT-specific minimum water stress scalar $wscal_{min}$. LPJmL-FIT simulates a large range of *LLs* as found in nature, and does not prescribe $wscal_{min}$ to enforce a specific phenology. Instead, LPJmL-FIT assigns each individual tree a random $wscal_{min}$ at establishment. This approach tests all conceivable $wscal_{min}$ values and supports individuals with the best adapted $wscal_{min}$ in a specific simulated environment (Data S1).

In conjunction with the *SLA*-*LL* trade-off, the effect of the randomized $wscal_{min}$ is that deciduous behavior is advantageous in dry regions because trees which do not invest much carbon into their leaves per unit dry mass (higher *SLA*) may shed them (lower *LL*) during the dry season. Conversely, evergreen behavior is advantageous in wet regions since the longer *LL*s allow achieving a constant carbon gain from photosynthesis throughout the year.

b.) The trade-off between *SLA* and the maximum carboxylation capacity of Rubisco (*Vcmax*) mediated by N_{area}

Empirical evidence shows a strongly positive relationship between a leaf's nitrogen content and its photosynthetic capacity (Field & Mooney, 1982; Reich *et al.,* 1994). Interconnected with *SLA* these leaf traits are part of the LES (Wright *et al.,* 2004) and introduce an additional source of variability in the spectrum of tree growth strategies of LPJmL-FIT.

Trees with high *SLA* not only have higher nitrogen content per unit mass, but also a higher photosynthetic nitrogen use efficiency (PNUE = rate of photosynthesis/amount of leaf nitrogen) (Poorter & Evans, 1998) as relatively more leaf nitrogen is invested into the photosynthetically active molecular structures within the chloroplasts (Evans & Seemann, 1989). On an area basis, however, thicker leaves with lower *SLA* have a higher photosynthetic capacity per area than thin leaves with high *SLA*.

Standard LPJmL ignores these functional relationships between *SLA*, nitrogen content and photosynthetic rates. Photosynthesis of PFTs is explicitly calculated depending on temperature, atmospheric CO_2 concentration, photosynthetically active radiation (*PAR*) and water availability (Farquhar *et al.,* 1980; Haxeltine & Prentice, 1996). One crucial variable in standard LPJmL's photosynthesis calculation is the maximum carboxylation rate of RUBISCO per leaf area ($Vcmax_{area}$),which is calculated on a daily basis (Sitch *et al.,* 2003).

In LPJmL-FIT, we account for the influence of *SLA* on N_{area} and the influence of N_{area} on photosynthetic capacity by introducing an *SLA* dependent N_{area} and a N_{area} dependent $Vcmax_{area}$ (Data S1).

c.) Trade-off between wood density (*WD*) and mortality

Wood density (*WD*) is a species-specific key trait determining the carbon storage capacity per unit volume as tree stems constitute about 2/3 of the aboveground tree biomass (Segura & Kanninen, 2005). Apart from affecting vegetation carbon, *WD* also influences the forest's age structure and maximum tree heights (Iida *et al.,* 2012).

In LPJmL standard, wood density (*WD*) is a constant parameter for all tree PFTs. LPJmL-FIT now varies *WD* because several mechanisms have been empirically established which link higher *WD* to higher construction costs and lower growth rates, but greater resistance against mechanical and drought stress (Baker *et al.,* 2004; Chao *et al.,* 2008; Chave *et al.,* 2006; Kraft *et al.,* 2008; Markesteijn *et al.,* 2011) and therefore, overall lower mortality (Anten & Schieving, 2010; Kraft *et al.,* 2010; Niklas & Spatz, 2010; Swenson & Enquist, 2007). Analogously to the leaf economics spectrum (LES) (Wright *et al.,* 2004), the stem economics spectrum (SES) links *WD*-dependent traits with particular growth strategies (Baraloto *et al.,* 2010; Chave *et al.,* 2009). *WD* is mechanistically separated in LPJmL-FIT from the traits involved in the LES (Data S1), because leaf and stem trade-offs operate largely independently (Baraloto *et al.,* 2010). We incorporated the *WD*-mortality trade-off using an equation derived by King et al. (2006) which assigns a *WD*-dependent annual mortality rate $mort_{WD}$ to each individual tree at tree establishment. $mort_{WD}$ is then used as the maximum of the growth efficiency dependent mortality from standard LPJmL (Data S1). Whilst a high *WD* decreases the growth rate of an individual, it also decreases the performance related mortality. Therefore a high *WD* tree generally grows slower, but also lives longer. This trade-off enables many different *WD*s to establish and therefore balances the variety of coexisting *WD*s.

Trait variability corridor

To conserve the natural variability of plant trait interrelations, we introduce the novel concept of a trait variability corridor in LPJmL-FIT which we apply to the log-log-*SLA*-*LL* regression (Fig. S5). Each value of an independent variable can now yield a range of values for the dependent variable, and within this range each value is assigned a certain probability. The range and probabilities are determined by normal distributions with a mean μ_α equal to the outcome of the original regression function and a standard deviation σ_α equal to half of the 50% prediction bounds of the original regression (Fig. S5). This approach is used at tree establishment when each sapling is assigned parameters which are drawn from the trait space within the trait variability corridor (see next section). We only applied this approach to the *SLA*-*LL* regression, because the introduced variability propagates to the derived trait values under the assumption that *SLA*, *LL*, N_{area} and Vc_{max} are interconnected directly or indirectly via the trade-offs of the LES.

Assignment of trait values to tree individuals

Each individual tree obtains a unique set of the trait values for *SLA*, *LL, WD,* N_{area}, $Vcmax_{area}$ and $wscal_{min}$ (Fig. 1). To obtain these sets, we first fit a probability density function (pdf) of a log-normal distribution (Data S1; Fig. S6) to the worldwide *SLA* recordings of broadleaved trees in the TRY database (Kattge *et al.,* 2011). The range between the 1 and 99% percentiles of this pdf determines the *SLA* range tested in LPJmL-FIT (*SLA* = 2.25-27mm^2 mg^{-1}). Within this range, 100 uniformly distributed *SLA* values determine the spectrum of 100 possible plant types regarding *SLA* (Fig. S6). According to the empirically based regression functions, each *SLA* value then leads to the calculation of a particular *LL* (Data S1 Eq. 1), N_{area} (Data S1 Eq. 2) and $Vcmax_{area}$ (Data S1 Eq. 3). We apply the trait variability corridor to the calculation of *LL*. Analogously to *SLA*, the potential range of *WDs* between 0.14 and 1.3g cm^{-3} was calculated from the PDF of the empirical *WD* distribution. Whereas the *SLA* and *WD* ranges were derived from empirically observed trait variation in the TRY database, the possible values of the minimum water scalar $wscal_{min}$ fall between 0 and 1. From within this range $wscal_{min}$ values are drawn randomly assuming a uniform distribution. The resulting 100 unique sets of trait values are assigned to respective 100 new tree saplings every 5 simulation years.

1.2 Vegetation dynamics

In LPJmL-FIT, 50 simulation patches each 100m² in size are introduced into each grid cell (Fig. S7). Within each patch individual trees are simulated. Each individual tree is a representative of a certain plant type. All plant types are allowed to grow in each patch. Resulting tree communities are scaled up to cover half-degree grid cells.

Light competition of individual trees

The basic light competition scheme is adapted from Smith *et al.* (2001) as in LPJ-GUESS. Within a patch, light competition occurs in distinct canopy layers each 100m² in size according to the patch area. The locations of these layers are prescribed starting at the maximum tree height (50m) followed by additional layers every 2m down to a height specific bole height, but not lower than 2m. Tree bole height is a yearly calculated variable depending on tree height (Thonicke *et al.,* 2010). If a tree is smaller than 2m (e.g. true for saplings), a respective fraction of its leaf mass is transferred to the first leaf layer where photosynthesis is possible (Fig. 1). An additional bottom layer enables the C3- and C4-grass PFTs of standard LPJmL to establish. Trees pass through the canopy layers during growth and distribute their leaf mass equally to the amount of layers they have reached above their bole height. The total amount of leaf area within each leaf layer determines the fraction of absorbed photosynthetic active radiation ($fAPAR_{Layer}$) according to the Lambert-Beers law (Data S1).

1.3 Output

Output trait distributions and trait maps

For the key traits *SLA*, *LL*, and *WD*, we fitted log-normal probability density functions (PDFs) to the trait distributions simulated in each grid cell in the Amazon Region. The distributions were fitted with the same type of probability density function (log-normal distribution) as was used for fitting the empirical TRY histograms. The investigated model output comprises averaged data from the last 600 out of 900 simulation years, since a 300 year initial phase was sufficient for trait distributions to reach equilibrium. Trait and trait variability maps were compiled by plotting the expectation value E and scale parameter σ of each log-normal PDF within each grid cell in the Amazon Region (Data S1).

For evaluation, E is the most common trait value, while σ is a measure of trait variability. We chose E, because trait expectation values are important for the magnitude of ecosystem processes, whereas σ determines the variety of viable growth strategies and may therefore be used as an indicator of the forest's capacity to adapt to environmental change (Isbell *et al.,* 2011; Mori *et al.,* 2013).

Output vegetation carbon

Carbon stored in the vegetation (gC m^{-2}) for the Amazon region was derived from LPJmL-FIT output data by averaging vegetation carbon in each grid cell across all surviving tree individuals including the grass PFTs over the last 600 years of the simulation.

1.4 Modelling protocol

Environmental drivers

Simulations are carried out for the Amazon basin. The model is driven by monthly climate data (temperature, precipitation, cloudiness, and number of wet days) from the CRU TS 3.10 compiled by the Climate Research Unit (Harris *et al.,* 2013). These are calculated on high-resolution (0.5° × 0.5°) grids which are based on an archive of monthly mean temperatures (Mitchell & Jones, 2005). To reach an equilibrium state of the vegetation, climate data from 1961-1990, which are interpolated to a daily time step, are constantly repeated for 900 years. The interval of 1961-1990 is chosen because the accuracy of input data for the Amazon basin is better than in previous years. To exclude CO_2-fertilization effects, the atmospheric CO_2 concentration is kept constant at the pre-industrial level of 288 ppm. Soil input data is based on the updated hydrology scheme for standard LPJmL (Schaphoff *et al.,* 2013). The soil types remain constant over time as we do not aim to disentangle climate and soil effects on trait distributions.

Three modelling experiments A-C reveal the effects of different model complexity on trait distributions and vegetation carbon.

Simulated experiments A-C

Experiment A. This simulation includes all three trade-offs listed above. The trait variability corridor is applied to the *SLA-LL* trade-off. We hypothesize that incorporating key traits and their trade-offs in a mechanistic framework successfully predicts observed plant trait distributions along a climatic gradient of the Amazon region (e.g. precipitation patterns and seasonality; Fig. S9) as well as vegetation carbon stocks which should fall in the observed ranges.

Experiment B. In this simulation we exclude the trait variability corridor of the *SLA-LL* trade-off, and use paired input values that were strictly derived from the *SLA*-*LL* regression function. We hypothesize that the resulting trait distributions should reflect a tree community with less diversity in functional traits because a large part of the natural variability is excluded from the trait space.

Experiment C. In addition to the changes made in experiments A and B, this experiment excludes the trade-off between *SLA* and *LL* and each tree is assigned a random *LL* within the *LL* range resulting from Eq. 1. We expect that without this essential trade-off, the resulting *SLA* and *LL* trait distributions should be shifted towards the thinner leaves with high leaf longevities, because both features increase the competitiveness.

Computational intensiveness

Simulations of LPJmL-FIT have relatively high computational costs compared to standard LPJmL. LPJmL-FIT accounts for light competition within the canopy as a compromise between the traditional PFT-representation (average individual approach) and representing individual trees with single stems and leaves in a spatially explicit manner. Diversifying former constant plant traits requires simulating a high number of different individuals. Under the settings described in this work, 900 year simulation years of the Amazon region take 3-4 days on 256 central processing units.

1.5 Model validation

Trait distributions

Simulated local trait distributions are evaluated at 12 selected locations (Fig. S8) where sufficient TRY data is available. We compare the expectation value E and the scale parameter σ of the fitted probability density functions (log-normal) of TRY data vs. LPJmL-FIT output to determine the difference between empirical vs. modeled trait distributions for *SLA*. Moreover, we calculate the percentage overlap (*ov*) of the two (empirical vs. modeled) probability density functions within the investigated SLA range (Data S1). This strategy has the advantage of comparing local distributions which contain information on both trait abundances and ranges instead of mean values. We focused on *SLA*, because this was the only trait where TRY offered sufficient empirical data for several locations in the Amazon region making location-specific model validation possible. Moreover, *SLA* distributions are representative for the other variable leaf traits as they are derived from *SLA* in LPJmL-FIT.

Vegetation carbon

Modeled vegetation carbon is compared to vegetation carbon estimates and associated uncertainties for the Amazon region based on remote sensing (Saatchi *et al.,* 2011) corrected for vegetation carbon of herbaceous cover (Carvalhais *et al.,* 2014).

Results

Comparing the experiments A-C at specific test locations

We show detailed results for 4 (L1-L4) out of 12 (L1-L12) validation locations (cf. Methods, Fig. S8). The complete results for all 12 locations are given in the SI (Table S1-S2, Fig. S10-S13).

In **experiment A** with the trait variability corridor included, the empirical and modeled distributions of *SLA* (Fig. 2a-h, Fig. S10-11) and their fitted log-normal probability functions (Fig. 2i-m, Fig. S12) agree very well at all 4 locations. The 4 selected sites L1-L4 (all 12 sites L1-L12) show a mean overlap between the modeled and observed PDFs of 88% (83%) with a

0.3-12.6% (0.3-23.7%) and 2.6-30.1% (1.5-31.5%) range of absolute difference between modeled and observed values of *E* and the scale parameter *σ*, respectively (Table S1, S2). The variability in *SLA*s as indicated by *σ* is largest in experiment A.

In **experiment B** the correlation corridor is not applied. Excluding the natural variability of the *SLA-LL* trade-off decreases the viable range of *SLAs* able to survive and compete successfully at a given location within a particular simulated environment. *E* values of *SLA* are shifted towards the lower *SLA* range and the respective distributions are narrower than in experiment A indicated by a smaller *σ* (Fig. 3, Fig. S13). The 4 selected sites L1-L4 (all 12 sites L1-L12) show a mean overlap of 63% (66 %) between the modeled and observed PDFs (Table S2, Fig. S13).

In **experiment C** the *SLA-LL* trade-off is excluded. The resulting *SLA* distribution is shifted strongly towards an unrealistically high range. The resulting *SLA* histograms do not follow a log normal distribution. The fitted PDFs increase exponentially towards the higher *SLA*s (Fig. 3, Fig. S13). Consistently, the 4 selected sites L1-L4 (all 12 sites L1-L12) show a mean overlap of 4% (5 %) between the modeled and observed PDFs (Table S2, Fig. S13).

Overall, the comparison of the experiments A-C indicates that the modeled *SLA* distributions strongly depend on the *SLA-LL* trade-off and the trait variability corridor (Fig. 3, S13). Whilst the trade-off itself constrains *SLA* distributions to the biological realistically range, the trait variability corridor ensures that establishing phenotypes cover this range.

Trait maps simulated for the Amazon region

The geographical pattern of specific leaf area (*SLA*) based on experiment A (Fig. 4) shows low expected *SLA* values in the North-Western wetter parts of the Amazon and high *SLAs* in the

South-Eastern drier parts of the Amazon region (Fig. 4a). This indicates that a combination of low *SLA* and high *LL*, which is characteristic for an evergreen phenology, is the most successful growth strategy in wet per-humid regions, whereas deciduous species with high *SLA* and low *LL* establish in dry regions with stronger rainfall seasonality. The variability in *SLA* (as indicated by the σ of the *SLA* probability density functions) is higher in drier and more seasonal areas (Fig. 4b). This indicates higher trait diversity in dry areas because of greater environmental variability.

The geographical patterns of leaf longevity (*LL*) (Fig. 4c) and *SLA* (Fig. 4a) are approximately inverted because *SLA* and *LL* are negatively correlated by the *SLA-LL* trade-off. Higher *LLs* are found in wetter per-humid areas because evergreen trees do not suffer from water stress (Fig. 4c). Such trees have *LLs* > 14 months, while deciduous trees in dry regions have *LLs* < 12 months, because they drop their leaves during the dry season. As for *SLA*, the σ of the *LL* distribution (Fig. 4d) is higher in the drier, more seasonal areas.

The geographical pattern of wood density (*WD*) (Fig. 4e) differs from the other two traits in that it does not represent a clear North-West to South-East gradient, but rather shows a crescent-shaped distribution. Highest *WD* values are found in the driest, most seasonal regions at the fringes of the Amazon, e.g. in the South, but also in wet regions in the Northwest with low intra-annual variability in precipitation (Fig. 4e).

Carbon stocks in the vegetation

In experiment A, vegetation carbon (Fig. S14) of 79% (41%) of all grid cells falls within the 5-95% (25-75%) uncertainty percentile range of one of the most recent and detailed map of vegetation carbon for the Amazon region (Saatchi *et al.,* 2011). Over- and underestimation of vegetation carbon are well- balanced with a mean difference of 0.11 and a standard deviation of

+/- 4.93 kgC m^{-2} across all grid cells between LPJmL-FIT and mean observed values. Excluding the trait variability corridor in experiment B not only reduces diversity of *SLA* (cf. Fig. 2), but also reduces the average vegetation carbon of the whole study area by 15% compared to experiment A (Fig. S14). In experiment B, vegetation carbon appears generally underestimated with the mean absolute difference of -1.75 and a standard deviation of +/- 4.79kgC m^{-2} across all grid cells between LPJmL-FIT and observed mean values.

Discussion

This study demonstrates a generalizable approach to a.) improve the representation of functional diversity in a DGVM by incorporating empirically-based trait distributions, and b.) employ a mechanistic framework of trade-offs to enable the coexistence of uniquely parameterized tree individuals with realistic growth strategies as defined by their trait combinations. A major advance of the individual- and trait-based DGVM LPJmL-FIT model is that the uniform input of trait values ensures that each trait combination gets the same chance to establish in a certain location. This flexible parameterization method avoids the pre-selection of tree types by bioclimatic limits as well as the model-specific calibration of plant traits. As a result, LPJmL-FIT replaces PFTs with numerous plant types representing functional spectra instead of constant plant parameters.

The study design with three simulated experiments A-C provides new insight into the mechanisms and selective forces shaping modeled and natural trait distributions in tree communities with different levels of functional diversity along a climatic gradient. Only the simulation **experiment A** with all trade-offs and the trait variability corridor included successfully reproduces empirical leaf trait distributions and vegetation carbon. Two further experiments B-C which lack functional components of the *SLA-LL* trade-off fail to do so. Here we first discuss the modelling implications, and then the ecological implications of this study.

Continuum of tree growth strategies replaces PFTs

From the climate of wetter and less seasonal tropical rainforests to the climate of drier and more seasonal closed and open dry deciduous forests, LPJmL-FIT produces a continuous gradient of tree growth strategies, replacing the strict classification of the "evergreen" and "raingreen" tropical broadleaved tree PFTs.

The results of experiment A show a large trait diversity in heterogeneous environments which implies that the *SLA-LL* trade-off has a decisive influence on the realized functional diversity in LPJmL-FIT as quantified by the expectation value E and width (scale parameter σ) of the modeled trait distributions. For example, the model predicts a high trait diversity at the fringes of the Amazon (Fig 4, right panels), where drought-avoiding deciduous species and drought-tolerant evergreen species coexist (Markesteijn & Poorter, 2009). Here, niche differentiation (Macarthur & Levins, 1967) due to climatic variability (seasonal and inter-annual) leads to coexistence of more growth strategies (Mori *et al.*, 2013; Sterk *et al.*, 2013). This suggests that climatic variability acts as a major driver shaping the realized niche (McGill *et al.*, 2006) of trees. The resulting trait divergence is also observed in natural communities (Brousseau *et al.*, 2013; Laurans *et al.*, 2012; Pillar *et al.*, 2009) where niche separation in a heterogeneous environment prevents competitive exclusion. The large trait variation should also make forests more resilient to environmental change due to higher response diversity (Mori *et al.*, 2013). Other studies have predicted that increased droughts could lead to the replacement by savanna vegetation (Hirota *et al.*, 2011; Nobre & Borma, 2009), or even forest collapse (Cox *et al.*, 2000; Cox *et al.*, 2013; Phillips *et al.*, 2009). LPJmL-FIT provides a tool to test which outcome is more likely in dependence of functional diversity, especially at the fringes of the Amazon, where climatic extremes are now more commonly observed (Marengo *et al.*, 2011; Saatchi *et al.*, 2013).

Conversely, a lower σ for all considered leaf and stem traits is simulated in areas with low climatic variability where trait convergence (Shipley *et al.*, 2006) occurs due to environmental filtering. Here, our model predicts a lower diversity of *SLA* and *LL* in the Northwestern Amazon, despite the high observed species diversity in this area (Baker *et al.*, 2014; ter Steege *et al.*, 2003). Due to functional redundancy, plant trait diversity cannot be directly translated into species diversity. However, the model results suggest that the lower plant trait diversity in this area may render it especially vulnerable to climatic changes.

Overall, the modeled trait distributions for *SLA* are very similar in expectation value *E* and scale parameter σ to the empirically-derived ones at all 12 tested locations in experiment A (mean overlap of PDFs: 86.7%, cf. Fig. 2, Fig. S12, and Table S1-2). The key to this successful model approach is that LPJmL-FIT selects for the best adapted growth strategies under different environmental conditions so that tree individuals optimize gains from photosynthesis per gram carbon investment into their leaves.

All viable growth strategies are based on trait combinations which lie within a multidimensional trait space constrained by trade-offs. Higher carbon investment per leaf area (lower *SLA*) is connected with higher possible carbon return time (*LL*) and higher possible return rate ($Vcmax_{area}$). These trade-offs enable a continuum between the extremes of short-lived, thin and less dense leaves and thicker, long-lived leaves as implied by the LES. Without this continuum, DGVMs are likely to misrepresent the seasonality of tree phenology and may therefore fail to predict future responses of forests to climate change (Richardson *et al.*, 2013). By including these trade-offs with the trait variability corridor and randomizing the threshold value for leaf abscission (*minwscal*) in LPJmL-FIT, we have achieved to reproduce the observed continuum of phenological strategies from evergreen to raingreen trees. This is a considerable advance over the simplified representation of phenology in existing DGVMs which prescribe either evergreen or deciduous PFTs.

Using the successful modelling approach from experiment A to model *SLA* distributions across the entire Amazon region, we find that the *SLA* expectation values agree well with the SLA map from Castanho *et al.* (2013) which interpolates field data. Few empirical data are available for the basin-wide validation of the modeled leaf longevity (*LL*). Independent data on estimated leaf longevities (Caldararu *et al.*, 2011) based on satellite images of the leaf area index from the MODIS product series (MOD15) support our simulated pattern with high *LLs* in the northwestern part of the Amazon region, and lower *LLs* in the southeastern part.

The northwestern part of the Amazon is characterized by high rainfall and irradiation as well as low climatic variability (Fig. S9). Here, the simulated *SLAs* are lowest and the most abundant *LLs* are >14 months. The favorable and comparatively stable growing conditions throughout the year promote the growth of trees with high *LLs*, since leaf shedding due to seasonal drought is not necessary. A high *LL* improves the carbon balance, increasing the competitiveness of an individual. A corresponding, low *SLA* entails a high Vc_N which can compensate for the higher carbon investment per leaf area of thicker and/or denser leaves. Together these advantages let plant types with low *SLAs* prevail in high and aseasonal rainfall areas in our simulations. In contrast, slow-growing, drought resistant, long-lived trees with high *SLAs*, *LLs* <12 months, and high *WD* are more abundant in drier areas with higher climatic variability, e.g. in the eastern to southern parts of the Amazon region.

Generally, the *WD*-mortality trade-off enables to simulate a continuum of competing *WDs* because it counteracts the higher growth rates of trees with low *WD*. The continuous *WD* distribution is an advance over setting constant *WD* for all tree types and contributes to a reasonably good match of simulated vegetation carbon with remote sensing data (Saatchi *et al.*, 2011). This implies that the *WD*-mortality trade-off is important for modelling ecosystem functioning, as *WD* influences the carbon storage capacity of the forest (Malhi *et al.*, 2006; Stegen *et al.*, 2009).

More specifically, the modeled *WD* pattern generally reflects the observed gradient from drier (higher *WD*) to wetter (lower *WD*) areas in Chave *et al.* (2009). However, at sites with pronounced nutrient wash-out (e.g. Guyana shield), LPJmL-FIT simulates evergreen trees with low *WD*, although field observations show a stronger Northeast to Southwest gradient (Quesada *et al.*, 2012; ter Steege *et al.*, 2006). This is because the simulated trait distributions are a result of climatically forced forest communities under competition, whereas other factors influencing tree growth such as nutrient availability (Quesada *et al.*, 2012; Fisher *et al.*, 2012) are still being ignored. In LPJmL-FIT, dry and seasonal climates as at the fringes of the Amazon promote higher *WDs and* wider *WD*-distributions because a relatively low growth efficiency promotes trees with high *WD*, reflecting their physiological advantage under water stress (Data S1 Eq. 6-7). In contrast, relatively high and constant annual rainfall as in the Northwestern part of the Amazon leads to a low growth efficiency-related mortality for all simulated tree types. In such areas, *E* values of *WDs* are intermediate to high because trees may invest carbon both into higher *WD* and into height growth at the same time. Notably, the constant rainfall also decreases the range of the *WD* distributions (Fig. 4f). In climates with intermediate rainfall and high seasonality as in the central and eastern part of the Amazon, the *E* values of *WD* are lowest because the two mechanisms promoting higher *WD* as described above are less effective.

Trait corridors enhance the number of growth strategies and the performance of tree individuals in trait-based models

Experiment B excludes the trait variability corridor around the *SLA*-*LL* trade-off. The corridor broadens the possible range of trait combinations at establishment time and is therefore essential to enlarge the width of the resulting trait distributions in the model. Within the spectrum of possible trait combinations in experiment A, there are combinations which outperform those in experiment B. In general, the trait variability corridor produces tree individuals with a higher performance, because trees with a certain *SLA* can adapt a variety of *LLs*, therefore partially capturing the variability within the *SLA*-*LL* trade-off. The magnitude and direction of this trait offset depends on the local environmental conditions. Hence, a higher trait variability as model input and a resulting higher adaptability leads to more productivity and an overall better C-balance of trees in LPJmL-FIT. This result suggests that the natural variability around empirically-based linear regressions of traits should be incorporated in trait-based models, which contrasts sharply with the fixed PFTs in most DGVMs.

Inclusion of trade-offs is essential to provide ecological realism

Experiment C completely excludes the *SLA*-*LL* trade-off. The resulting *SLA* expectation values become unrealistically high. High *SLAs* are much more competitive than lower ones in all regions, because they invest less carbon into their leaves per area (thin or less dense leaves), while they are also able to maintain high *LL*s. Therefore, they achieve unrealistically high returns from photosynthesis. This result implies that just varying trait parameters without constraining them by an ecophysiologically motivated trade-off is insufficient to replace the fixed PFT approach and fails to reproduce natural patterns of plant trait diversity and indicators of ecosystem functioning.

Potential of LPJmL-FIT to model the effects of functional diversity on ecosystem functioning

Up to now, hypotheses about the links between B-EF could neither be tested systematically nor quantitatively established with DGVMs. LPJmL-FIT advances in this direction because it improves the representation of functional diversity by combining three modelling strategies: a.) the gap model approach with simulation of individual trees which enables unique trait combinations and local competition for resources, b) parameter assignment to these trees based on empirical trait ranges publicly available from the TRY plant trait database (Kattge *et al.,* 2011), and c.) the empirically-grounded constriction of the trait parameter space by the implemented trade-offs and the trait variability corridor based on the LES. This methodology directly address several calls (Adler *et al.*, 2013; Quillet *et al.*, 2010; Webb *et al.*, 2010) to better quantify the influence of continuous multiple traits on ecosystem functions by testing their functional redundancy and complementarity with empirical data and vegetation models .The combination of a strong theoretical core, mechanistic relationships, and the empirically-derived knowledge on trait correlations makes LPJmL-FIT a powerful modeling tool for testing of leading BEF-related hypotheses, e.g. the insurance hypothesis (Yachi & Loreau, 1999; Walker, 1992) and the mass-ratio hypothesis (Grime, 1998), at different spatial scales.

As a future outlook, LPJmL-FIT could be extended to needle-leaved and herbaceous plants to model other natural ecosystems. For forests, LPJmL-FIT lends itself to simulate the effects of different logging schemes on the trait diversity of trees and the carbon cycle in exchange with the atmosphere. LPJmL-FIT may also predict the effects of global warming and CO_2 fertilization on individual tree physiology to reduce model uncertainty (Rammig *et al.,* 2010) and to better understand processes leading to biodiversity loss, e.g. by identifying ecological tipping points in scenarios of global change.

Acknowledgements

We thank Nuno Carvalhais and Matthias Forkel from the Max Planck Institute for Biogeochemistry (Jena, Germany), Jörg Asmus (University of Bergen, Norway), and Jasmin Joshi (University of Potsdam, Germany) for lively discussions about an earlier version of this manuscript. Many thanks to Dennis Drechsler for helping with the figure design. The research leading to these results has received funding from the European Union Seventh Framework Programme (FP7/2007-2013) under grant agreement n° 283093 – The Role Of Biodiversity In climate change mitigatioN (ROBIN). We thank Christopher Baraloto and one anonymous reviewer for constructive comments on an earlier version of the manuscript. The study has been supported by the TRY initiative on plant traits (http://www.try-db.org). The TRY initiative and database is hosted, developed and maintained by J. Kattge and G. Bönisch (Max Planck Institute for Biogeochemistry, Jena, Germany). TRY is/has been supported by DIVERSITAS, IGBP, the Global Land Project, the UK Natural Environment Research Council (NERC) through its program QUEST (Quantifying and Understanding the Earth System), the French Foundation for Biodiversity Research (FRB), and GIS "Climat, Environnement et Société" France.

Reference List

Anten NP, Schieving F (2010) The Role of Wood Mass Density and Mechanical Constraints in the Economy of Tree Architecture. *The American Naturalist,* **175,** 250-260.

Atkin OK, Schortemeyer M, McFarlane N, Evans JR (1999) The response of fast- and slow-growing Acacia species to elevated atmospheric CO2: an analysis of the underlying components of relative growth rate. *Oecologia,* **120,** 544-554.

Baker TR, Phillips OL, Malhi Y, et al., (2004) Variation in wood density determines spatial patterns in Amazonian forest biomass. *Global Change Biology,* **10,** 545-562.

Balvanera P, Pfisterer AB, Buchmann N, He JS, Nakashizuka T, Raffaelli D, Schmid B (2006) Quantifying the evidence for biodiversity effects on ecosystem functioning and services. *Ecology Letters,* **9,** 1146-1156.

Baraloto C, Timothy Paine CE, Poorter L, et al., (2010) Decoupled leaf and stem economics in rain forest trees. *Ecology Letters,* **13,** 1338-1347.

Bondeau A, Smith PC, Zaehle S, et al., (2007) Modelling the role of agriculture for the 20th century global terrestrial carbon balance. *Global Change Biology,* **13,** 679-706.

Bugmann H (2001) A review of forest gap models. *Climatic Change,* **51,** 259-305.

Campbell C, Atkinson L, Zaragoza-Castells J, Lundmark M, Atkin O, Hurry V (2007) Acclimation of photosynthesis and respiration is asynchronous in response to changes in temperature regardless of plant functional group. *New Phytologist,* **176,** 375-389.

Cardinale BJ, Duffy JE, Gonzalez A, et al., (2012) Biodiversity loss and its impact on humanity. *Nature,* **486,** 59-67.

Carvalhais N, Forkel M, Khomik M, et al., (2014) Global covariation of carbon turnover times with climate in terrestrial ecosystems. pp. 213-217.

Castro-Diez P, Puyravaud JP, Cornelissen JHC, Villar-Salvador P (1998) Stem anatomy and relative growth rate in seedlings of a wide range of woody plant species and types. *Oecologia,* **116,** 57-66.

Chabot BF, Hicks DJ (1982) The Ecology of Leaf Life Spans. *Annual Review of Ecology and Systematics,* **13,** 229-259.

Chao KJ, Phillips OL, Gloor E, Monteagudo A, Torres-Lezama A, Mart+¡nez RV (2008) Growth and wood density predict tree mortality in Amazon forests. *Journal of Ecology,* **96,** 281-292.

Chave J, Muller-Landau HC, Baker TR, Easdale TA, Ter Steege H, Webb CO (2006) Regional and phylogenetic variation of wood density across 2456 neotropical tree species. *Ecological Applications,* **16,** 2356-2367.

Chave J, Coomes D, Jansen S, Lewis SL, Swenson NG, Zanne AE (2009) Towards a worldwide wood economics spectrum. *Ecology Letters,* **12,** 351-366.

Cornelissen JHC (1996) An experimental comparison of leaf decomposition rates in a wide range of temperate plant species and types. *Journal of Ecology,* **84,** 573-582.

Cornelissen JHC, Cerabolini B, Castro-Diez P, et al., (2003) Functional traits of woody plants: correspondence of species rankings between field adults and laboratory-grown seedlings? *Journal of Vegetation Science,* **14,** 311-322.

Cornelissen JHC, Diez PC, Hunt R (1996) Seedling growth, allocation and leaf attributes in a wide range of woody plant species and types. *Journal of Ecology,* **84,** 755-765.

Cornelissen JHC, Quested HM, Gwynn-Jones D, et al., (2004) Leaf digestibility and litter decomposability are related in a wide range of subarctic plant species and types. *Functional Ecology,* **18,** 779-786.

Cornwell WK, Cornelissen JHC, Amatangelo K, et al., (2008) Plant species traits are the predominant control on litter decomposition rates within biomes worldwide. *Ecology Letters,* **11,** 1065-1071.

Cox PM, Betts RA, Jones CD, Spall SA, Totterdell IJ (2000) Acceleration of global warming due to carbon-cycle feedbacks in a coupled climate model. *Nature,* **408,** 184-187.

Cox PM, Pearson D, Booth BB, Friedlingstein P, Huntingford C, Jones CD, Luke CM (2013) Sensitivity of tropical carbon to climate change constrained by carbon dioxide variability. *Nature,* **494,** 341-344.

Diaz S, Cabido M (2001) Vive la difference: plant functional diversity matters to ecosystem processes. *TRENDS in Ecology & Evolution,* **16,** 646-655.

Diaz S, Hodgson JG, Thompson K, et al., (2004) The plant traits that drive ecosystems: Evidence from three continents. *Journal of Vegetation Science,* **15,** 295-304.

Evans JR, Seemann JR (1989) The allocation of protein nitrogen in the photosynthetic apparatus: costs, consequences, and control. In:*Photosynthesis* (ed Briggs WR), Alan R Liss Inc., New York, USA.

Farquhar GD, Caemmerer SV, Berry JA (1980) A Biochemical-Model of Photosynthetic Co2 Assimilation in Leaves of C-3 Species. *Planta,* **149,** 78-90.

Field C, Mooney HA (1982) The photosynthesis-nitrogen relationship in wild plants. In:*On the economy of plant form and function* (ed Givnish TJ), pp. 25-55. Cambridge University Press, Cambridge, UK.

Fonseca CR, Overton JM, Collins B, Westoby M (2000) Shifts in trait-combinations along rainfall and phosphorus gradients. *Journal of Ecology,* **88,** 964-977.

Freschet GT, Cornelissen JHC, van Logtestijn RSP, Aerts R (2010) Evidence of the 'plant economics spectrum' in a subarctic flora. *Journal of Ecology,* **98,** 362-373.

Fyllas NM, Gloor E, Mercado LM, et al., (2014) Analysing Amazonian forest productivity using a new individual and trait-based model (TFS v.1). *Geosci.Model Dev.Discuss.,* **7,** 1413-1452.

Fyllas NM, Patino S, Baker TR, et al., (2009) Basin-wide variations in foliar properties of Amazonian forest: phylogeny, soils and climate. *Biogeosciences,* **6,** 2677-2708.

Garnier E, Lavorel S, Ansquer P, et al., (2007) Assessing the effects of land-use change on plant traits, communities and ecosystem functioning in grasslands: A standardized methodology and lessons from an application to 11 European sites. *Annals of Botany,* **99,** 967-985.

Gerten D, Schaphoff S, Haberlandt U, Lucht W, Sitch S (2004) Terrestrial vegetation and water balance - hydrological evaluation of a dynamic global vegetation model. *Journal of Hydrology,* **286,** 249-270.

Grime JP (1998) Benefits of plant diversity to ecosystems: immediate, filter and founder effects. *Journal of Ecology,* **86,** 902-910.

Gutierrez AG, Huth A (2012) Successional stages of primary temperate rainforests of Chiloe Island, Chile. *Perspectives in Plant Ecology Evolution and Systematics,* **14,** 243-256.

Harris I, Jones PD, Osborn TJ, Lister DH (2013) Updated high-resolution grids of monthly climatic observations GÇô the CRU TS3.10 Dataset. *International Journal of Climatology,* n/a.

Haxeltine A, Prentice IC (1996) BIOME3: An equilibrium terrestrial biosphere model based on ecophysiological constraints, resource availability, and competition among plant functional types. *Global Biogeochemical Cycles,* **10,** 693-709.

Hector A, Bagchi R (2007) Biodiversity and ecosystem multifunctionality. *Nature,* **448,** 188-1U6.

Hillebrand H, Matthiessen B (2009) Biodiversity in a complex world: consolidation and progress in functional biodiversity research. *Ecology Letters,* **12,** 1405-1419.

Hooper DU, Chapin FS, Ewel JJ, et al., (2005) Effects of biodiversity on ecosystem functioning: A consensus of current knowledge. *Ecological Monographs,* **75,** 3-35.

Hooper DU, Adair EC, Cardinale BJ, et al., (2012) A global synthesis reveals biodiversity loss as a major driver of ecosystem change. *Nature,* **486,** 105-108.

Iida Y, Poorter L, Sterck FJ, Kassim AR, Kubo T, Potts MD, Kohyama TS (2012) Wood density explains architectural differentiation across 145 co-occurring tropical tree species. *Functional Ecology,* **26,** 274-282.

Isbell F, Calcagno V, Hector A, et al., (2011) High plant diversity is needed to maintain ecosystem services. *Nature,* **477,** 199-U96.

Kattge J, Diaz S, Lavorel S, et al., (2011) TRY - a global database of plant traits. *Global Change Biology,* **17,** 2905-2935.

Kattge J, Knorr W, Raddatz T, Wirth C (2009) Quantifying photosynthetic capacity and its relationship to leaf nitrogen content for global-scale terrestrial biosphere models. *Global Change Biology,* **15,** 976-991.

Kikuzawa K (1995) The basis for variation in leaf longevity of plants. *Vegetatio,* **121,** 89-100.

Kikuzawa K, Lechowicz MJ (2011) Theories of leaf longevity. In:*Ecology of leaf longevity* pp. 41-56. Springer, Germany.

King DA, Davies SJ, TAN SYLV, Noor NSM (2006) The role of wood density and stem support costs in the growth and mortality of tropical trees. *Journal of Ecology,* **94,** 670-680.

Kitajima K, Poorter L (2010) Tissue-level leaf toughness, but not lamina thickness, predicts sapling leaf lifespan and shade tolerance of tropical tree species. *New Phytologist,* **186,** 708-721.

Kleyer M, Bekker RM, Knevel IC, et al., (2008) The LEDA Traitbase: a database of life-history traits of the Northwest European flora. *Journal of Ecology,* **96,** 1266-1274.

Kraft NJB, Metz MR, Condit RS, Chave J (2010) The relationship between wood density and mortality in a global tropical forest data set. *New Phytologist,* **188,** 1124-1136.

Kraft NJB, Valencia R, Ackerly DD (2008) Functional Traits and Niche-Based Tree Community Assembly in an Amazonian Forest. *Science,* **322,** 580-582.

Kurokawa H, Nakashizuka T (2008) Leaf herbivory and decomposability in a Malaysian tropical rain forest. *Ecology,* **89,** 2645-2656.

Laughlin DC, Leppert JJ, Moore MM, Sieg CH (2010) A multi-trait test of the leaf-height-seed plant strategy scheme with 133 species from a pine forest flora. *Functional Ecology,* **24,** 493-501.

Loreau M, Naeem S, Inchausti P, et al., (2001) Ecology - Biodiversity and ecosystem functioning: Current knowledge and future challenges. *Science,* **294,** 804-808.

Loveys BR, Atkinson LJ, Sherlock DJ, Roberts RL, Fitter AH, Atkin OK (2003) Thermal acclimation of leaf and root respiration: an investigation comparing inherently fast- and slow-growing plant species. *Global Change Biology,* **9,** 895-910.

Malhi Y, Aragão LEOC, Galbraith D, et al., (2009) Exploring the likelihood and mechanism of a climate-change-induced dieback of the Amazon rainforest. *Proceedings of the National Academy of Sciences,* **106,** 20610-20615.

Markesteijn L, Poorter L, Paz H, Sack L, Bongers F (2011) Ecological differentiation in xylem cavitation resistance is associated with stem and leaf structural traits. *Plant Cell and Environment,* **34,** 137-148.

McCann KS (2000) The diversity-stability debate. *Nature,* **405,** 228-233.

Medlyn BE, Badeck FW, De Pury DGG, et al., (1999) Effects of elevated [CO2] on photosynthesis in European forest species: a meta-analysis of model parameters. *Plant Cell and Environment,* **22,** 1475-1495.

Messier J, Mcgill BJ, Lechowicz MJ (2010) How do traits vary across ecological scales? A case for trait-based ecology. *Ecology Letters,* **13,** 838-848.

Mitchell TD, Jones PD (2005) An improved method of constructing a database of monthly climate observations and associated high-resolution grids. *International Journal of Climatology,* **25,** 693-712.

Mori AS, Furukawa T, Sasaki T (2013) Response diversity determines the resilience of ecosystems to environmental change. *Biological Reviews,* **88,** 349-364.

Morin X, Fahse L, Scherer-Lorenzen M, Bugmann H (2011) Tree species richness promotes productivity in temperate forests through strong complementarity between species. *Ecology Letters,* **14,** 1211-1219.

Naeem S, Thompson LJ, Lawler SP, Lawton JH, Woodfin RM (1994) Declining Biodiversity Can Alter the Performance of Ecosystems. *Nature,* **368,** 734-737.

Naeem S, Wright JP (2003) Disentangling biodiversity effects on ecosystem functioning: deriving solutions to a seemingly insurmountable problem. *Ecology Letters,* **6,** 567-579.

Niinemets U (2001) Global-scale climatic controls of leaf dry mass per area, density, and thickness in trees and shrubs. *Ecology,* **82,** 453-469.

Niklas KJ, Spatz HC (2010) Worldwide correlations of mechanical properties and green wood density. *American Journal of Botany,* **97,** 1587-1594.

Ogaya R, Penuelas J (2003) Comparative field study of Quercus ilex and Phillyrea latifolia: photosynthetic response to experimental drought conditions. *Environmental and Experimental Botany,* **50,** 137-148.

Ordonez JC, van Bodegom PM, Witte JPM, Bartholomeus RP, van Hal JR, Aerts R (2010) Plant Strategies in Relation to Resource Supply in Mesic to Wet Environments: Does Theory Mirror Nature? *American Naturalist,* **175,** 225-239.

Pavlick R, Drewry DT, Bohn K, Reu B, Kleidon A (2012) The Jena Diversity-Dynamic Global Vegetation Model (JeDi-DGVM): a diverse approach to representing terrestrial biogeography and biogeochemistry based on plant functional trade-offs. pp. 4627-4726.

Penuelas J, Sardans J, Llusia J, et al., (2010) Faster returns on 'leaf economics' and different biogeochemical niche in invasive compared with native plant species. *Global Change Biology,* **16,** 2171-2185.

Poorter H, Niinemets U, Poorter L, Wright IJ, Villar R (2009) Causes and consequences of variation in leaf mass per area (LMA): a meta-analysis. *New Phytologist,* **182,** 565-588.

Poorter H, Evans JR (1998) Photosynthetic nitrogen-use efficiency of species that differ inherently in specific leaf area. *Oecologia,* **116,** 26-37.

Poorter L, Bongers F (2006) Leaf traits are good predictors of plant performance across 53 rain forest species. *Ecology,* **87,** 1733-1743.

Poorter L, Wright SJ, Paz H, et al., (2008) Are functional traits good predictors of demographic rates? Evidence from five Neotropical forests. *Ecology,* **89,** 1908-1920.

Poulter B, Ciais P, Hodson E, Lischke H, Maignan F, Plummer S, Zimmermann NE (2011) Plant functional type mapping for earth system models. *Geoscientific Model Development,* **4,** 993-1010.

Prentice IC, Cramer W, Harrison SP, Leemans R, Monserud RA, Solomon AM (1992) A Global Biome Model Based on Plant Physiology and Dominance, Soil Properties and Climate. *Journal of Biogeography,* **19,** 117-134.

Preston KA, Cornwell WK, DeNoyer JL (2006) Wood density and vessel traits as distinct correlates of ecological strategy in 51 California coast range angiosperms. *New Phytologist,* **170,** 807-818.

Quested HM, Cornelissen JHC, Press MC, et al., (2003) Decomposition of sub-arctic plants with differing nitrogen economies: A functional role for hemiparasites. *Ecology,* **84,** 3209-3221.

Rammig A, Jupp T, Thonicke K, et al., (2010) Estimating the risk of Amazonian forest dieback. *New Phytologist,* **187,** 694-706.

Reich PB, Ellsworth DS, Walters MB, Vose JM, Gresham C, Volin JC, Bowman WD (1999) Generality of leaf trait relationships: A test across six biomes. *Ecology,* **80,** 1955-1969.

Reich PB, Oleksyn J, Wright IJ (2009) Leaf phosphorus influences the photosynthesis-nitrogen relation: a cross-biome analysis of 314 species. *Oecologia,* **160,** 207-212.

Reich PB, Tjoelker MG, Pregitzer KS, Wright IJ, Oleksyn J, Machado JL (2008) Scaling of respiration to nitrogen in leaves, stems and roots of higher land plants. *Ecology Letters,* **11,** 793-801.

Reich PB, Uhl C, Walters MB, Ellsworth DS (1991) Leaf Life-Span As A Determinant of Leaf Structure and Function Among 23 Amazonian Tree Species. *Oecologia,* **86,** 16-24.

Reich PB, Uhl C, Walters MB, Prugh L, Ellsworth DS (2004) Leaf demography and phenology in Amazonian rain forest: A census of 40 000 leaves of 23 tree species. *Ecological Monographs,* **74,** 3-23.

Reich PB, Walters MB, Ellsworth DS (1997) From tropics to tundra: Global convergence in plant functioning. *Proceedings of the National Academy of Sciences of the United States of America,* **94,** 13730-13734.

Reich PB, Walters MB, Ellsworth DS, Uhl C (1994) Photosynthesis-Nitrogen Relations in Amazonian Tree Species. I. Patterns among Species and Communities. *Oecologia,* **97,** 62-72.

Reiss J, Bridle JR, Montoya JM, Woodward G (2009) Emerging horizons in biodiversity and ecosystem functioning research. *Trends in Ecology & Evolution,* **24,** 505-514.

Reu B, Proulx R, Bohn K, Dyke JG, Kleidon A, Pavlick R, Schmidtlein S (2011a) The role of climate and plant functional trade-offs in shaping global biome and biodiversity patterns. *Global Ecology and Biogeography,* **20,** 570-581.

Reu B, Zaehle S, Proulx R, Bohn K, Kleidon A, Pavlick R, Schmidtlein S (2011b) The role of plant functional trade-offs for biodiversity changes and biome shifts under scenarios of global climatic change. *Biogeosciences,* **8,** 1255-1266.

Ruger N, Wirth C, Wright SJ, Condit R (2012) Functional traits explain light and size response of growth rates in tropical tree species. *Ecology,* **93,** 2626-2636.

Saatchi SS, Harris NL, Brown S, et al., (2011) Benchmark map of forest carbon stocks in tropical regions across three continents. *Proceedings of the National Academy of Sciences*.

Schaphoff S, Heyder U, Ostberg S, Gerten D, Heinke J, Lucht W (2013) Contribution of permafrost soils to the global carbon budget. *Environmental Research Letters,* **8,** 014026.

Scheiter S, Langan L, Higgins SI (2013) Next-generation dynamic global vegetation models: learning from community ecology. *New Phytologist,* **198,** 957-969.

Segura M, Kanninen M (2005) Allometric Models for Tree Volume and Total Aboveground Biomass in a Tropical Humid Forest in Costa Rica1. *Biotropica,* **37,** 2-8.

Shiodera S, Rahajoe JS, Kohyama T (2008) Variation in longevity and traits of leaves among co-occurring understorey plants in a tropical montane forest. *Journal of Tropical Ecology,* **24,** 121-133.

Shipley B (2002) Trade-offs between net assimilation rate and specific leaf area in determining relative growth rate: relationship with daily irradiance. *Functional Ecology,* **16,** 682-689.

Shipley B, Vu TT (2002) Dry matter content as a measure of dry matter concentration in plants and their parts. *New Phytologist,* **153,** 359-364.

Shipley B, Lechowicz MJ, Wright I, Reich PB (2006) Fundamental trade-offs generating the worldwide leaf economics spectrum. *Ecology,* **87,** 535-541.

Sitch S, Huntingford C, Gedney N, et al., (2008) Evaluation of the terrestrial carbon cycle, future plant geography and climate-carbon cycle feedbacks using five Dynamic Global Vegetation Models (DGVMs). *Global Change Biology,* **14,** 2015-2039.

Sitch S, Smith B, Prentice IC, et al., (2003) Evaluation of ecosystem dynamics, plant geography and terrestrial carbon cycling in the LPJ dynamic global vegetation model. *Global Change Biology,* **9,** 161-185.

Smith B, Prentice IC, Sykes MT (2001) Representation of vegetation dynamics in the modelling of terrestrial ecosystems: comparing two contrasting approaches within European climate space. *Global Ecology and Biogeography,* **10,** 621-637.

Sterck FJ, Poorter L, Schieving F (2006) Leaf traits determine the growth-survival trade-off across rain forest tree species. *American Naturalist,* **167,** 758-765.

Sterk M, Gort G, Klimkowska A, van Ruijven J, van Teeffelen AJA, Wamelink GWW (2013) Assess ecosystem resilience: Linking response and effect traits to environmental variability. *Ecological Indicators,* **30,** 21-27.

Suding KN, Lavorel S, CHAPIN FS, et al., (2008) Scaling environmental change through the community-level: a trait-based response-and-effect framework for plants. *Global Change Biology,* **14,** 1125-1140.

Swaine EK (2007) Ecological and evolutionary drivers of plant community assembly in a Bornean rain forest. Dissertation at Aberdeen University, School of Biological Sciences, UK.

Swenson NG, Enquist BJ (2007) Ecological and evolutionary determinants of a key plant functional trait: wood density and its community-wide variation across latitude and elevation. *American Journal of Botany,* **94,** 451-459.

Taylor AR, Chen HYH, VanDamme L (2009) A Review of Forest Succession Models and Their Suitability for Forest Management Planning. *Forest Science,* **55,** 23-36.

Thonicke K, Spessa A, Prentice IC, Harrison SP, Dong L, Carmona-Moreno C (2010) The influence of vegetation, fire spread and fire behaviour on biomass burning and trace gas emissions: results from a process-based model. *Biogeosciences,* **7,** 1991-2011.

Van Bodegom PM, Douma JC, Witte JPM, Ordoñez JC, Bartholomeus RP, Aerts R (2012) Going beyond limitations of plant functional types when predicting global ecosystem's atmosphere fluxes: exploring the merits of traits-based approaches. *Global Ecology and Biogeography,* **21,** 625-636.

van Ommen Kloeke AEE, Douma JC, Ordonez JC, Reich PB, Van Bodegom PM (2012) Global quantification of contrasting leaf life span strategies for deciduous and evergreen species in response to environmental conditions. *Global Ecology and Biogeography,* **21,** 224-235.

Verheijen LM, Brovkin V, Aerts R, et al., (2013) Impacts of trait variation through observed trait-climate relationships on performance of an Earth system model: a conceptual analysis. *Biogeosciences,* **10,** 5497-5515.

Violle C, Navas ML, Vile D, Kazakou E, Fortunel C, Hummel In, Garnier E (2007) Let the concept of trait be functional! *Oikos,* **116,** 882-892.

Walker BH (1992) Biodiversity and Ecological Redundancy. *Conservation Biology,* **6,** 18-23.

Westoby M, Falster DS, Moles AT, Vesk PA, Wright IJ (2002) Plant ecological strategies: Some leading dimensions of variation between species. *Annual Review of Ecology and Systematics,* **33,** 125-159.

Westoby M, Warton D, Reich PB (2000) The time value of leaf area. *American Naturalist,* **155,** 649-656.

Westoby M, Wright IJ (2006) Land-plant ecology on the basis of functional traits. pp. 261-268.

Willis CG, Halina M, Lehman C, Reich PB, Keen A, McCarthy S, Cavender-Bares J (2010) Phylogenetic community structure in Minnesota oak savanna is influenced by spatial extent and environmental variation. *Ecography,* **33,** 565-577.

Woodward FI, Kelly CK (1997) Plant functional types: towards a definition by environmental constraints. In:*Plant functional types: their relevance to ecosystem properties and global change* (eds Smith TM, Shuhart HH, Woodward FI), pp. 47-65. Cambridge University Press, Cambridge, UK.

Wright IJ, Ackerly DD, Bongers F, et al., (2007) Relationships among ecologically important dimensions of plant trait variation in seven Neotropical forests. *Annals of Botany,* **99,** 1003-1015.

Wright IJ, Reich PB, Westoby M, et al., (2004) The worldwide leaf economics spectrum. *Nature,* **428,** 821-827.

Wright SJ, Kitajima K, Kraft NJB, et al., (2010) Functional traits and the growth-mortality trade-off in tropical trees. *Ecology,* **91,** 3664-3674.

Xu LK, Baldocchi DD (2003) Seasonal trends in photosynthetic parameters and stomatal conductance of blue oak (Quercus douglasii) under prolonged summer drought and high temperature. *Tree Physiology,* **23,** 865-877.

Yachi S, Loreau M (1999) Biodiversity and ecosystem productivity in a fluctuating environment: The insurance hypothesis. *Proceedings of the National Academy of Sciences of the United States of America,* **96,** 1463-1468.

Supporting information

Additional Supporting Information may be found in the online version of this article:

Data S1. Additional information regarding standard LPJmL model description, trade-offs implemented in LPJmL-FIT, details of linear regressions, light competition scheme of individual trees in LPJmL-FIT, distribution fitting, calculation of probability density function overlap as well as 20 additional references are provided.

Table S1. Comparison of modeled vs. observed expected values *E* and scale parameter *sigma* based on probability density functions of *SLA* trait distributions across the Amazon region.

Table S2. Percentage overlap (*ov*) between probability density functions of modeled vs. observed *SLA*.

Fig. S1 Geographical origin of TRY data used to derive the tradeoffs of this study (Data S1 eq. 1, 2, 3). Blue circles indicate data of the *SLA-LL* regression (Data S1 eq. 1). Orange circles indicate the data of the SLA-N_{area} regression (Data S1 eq. 2). Cyan circles indicate data of the N_{area}-$Vcmax_{area}$ regression (Data S1 eq. 3).

Fig. S2. Regression of leaf longevity (*LL*) against specific leaf area (*SLA*).

Fig. S3. Regression of leaf nitrogen per leaf area (N_{area}) against specific leaf area (SLA).

Fig. S4. Regression of maximum carboxylation rate of RUBISCO enzyme per area measured at 25°C ($Vcmax_{\mathrm{area}25°}$) against leaf nitrogen per leaf area (N_{area}).

Fig. S5. Trait variability corridor of a regression between two exemplary traits.

Fig. S6. Sampling of *SLA* input values for LPJmL-FIT based on data from TRY.

Fig. S7. Visualization of LPJmL-FITs vegetation dynamics.

Fig. S8. Test locations L1-L12 where sufficient TRY data were available for fitting empirical

SLA distributions with probability density functions. Coordinates of sites (longitude, latitude): L1 (-60.75, -14.75); L2 (-60.25, -2.75); L3 (-76.25, -0.75); L4 (-69.25, -12.75); L5 (-77.75, -1.25); L6 (-67.26, 1.75); L7 (-51.25, -1.75); L8 (-61.25, -14.25); L9 (-68.25, -10.75); L10 (-72.75, -3.25); L11 (-44.75, -23.25); L12 (-79.75, 8.75).

Fig. S9. Precipitation patterns of input data used for all simulations in the Amazon region. a) Annual mean of the precipitation data. b) Mean annual standard deviation of the precipitation data.

Fig. S10. Histograms of *SLA* values from TRY database at the 12 test locations L1-L12 (cf. Fig. S8) throughout the Amazon region.

Fig. S11. Histograms of *SLA* values simulated in experiment A in LPJmL-FIT at the 12 selected test locations L1-L12.

Fig. S12. Probability density functions fitted to the *SLA* distributions from the TRY database and LPJmL-FIT in simulated experiment A at the 12 test locations L1-L12.

Fig. S13. Comparison between the probability density functions for the *SLA* distributions derived from simulated experiments A, B, and C, and the TRY database.

Fig. S14. Modeled vs. observed mean vegetation carbon (vegC) across the Amazon region.

Figure legends

Fig. 1: Flowchart of LPJmL-FIT. a.) Input: Parameter settings for individual trees are generated at tree establishment at the beginning of every 5th simulated year. A uniform distribution of input *SLA, WD and* $wscal_{min}$ values and the derived trait values for N_{area}, *LL*, and $Vcmax_{area}$ gives every possible trait combination within the parameter space the same chance to establish at a given location. b) Vegetation dynamics: Trees compete for light and water while passing through distinct canopy layers during growth. A bottom layer (0) represents the grass the C3- and C4-grass PFTs (see video visualization of model output under: http://www.pik-potsdam.de/~borissa/video; documentation in Fig. S7). The location of individual trees within a patch is not spatially explicit so that total leaf area within a canopy layer is mixed. c) Output: Individual trees above 5m in height and their respective trait combinations are recorded each year. More competitive trait combinations show a higher contribution to the growing data set. A histogram of the simulated trait distribution (e.g. *SLA*) is established from a sufficient number of patches and simulation years (cf. Methods). Local trait distributions enable to compile trait maps for a whole region.

Fig. 2: Top: Histograms of observed *SLA* values (broadleaved trees) from the TRY database (Kattge *et al.,* 2011) at four selected locations L1-L4 (cf. 4a). The number of observations for each panel is N = 86 (L1), N = 122 (L2), N = 119 (L3), and N = 143 (L4). Center: Histograms of simulated SLA values from experiment A at the same locations. The average number of trees per ha and year for each panel is N = 270 (L1), N = 164 (L2), N = 197 (L3), and N = 250 (L4). Simulated *SLA* distributions refer to trees > 5m in height and the last 600 out of 900 simulation years. Bottom: Comparison of probability density functions fitted to the distributions in the top and center panel for the same locations. The distributions of the observed *SLA*s in the TRY data

base (red) match closely with the simulated *SLA* distributions (black).

Fig. 3: Probability density functions of observed *SLA* distributions (black, solid line) from the TRY database (Kattge et al., 2011) in comparison to simulated experiments A (red), B (dashed), and C (dashed-dotted) at location L2 (cf. Fig. 4 for a map of all locations). For experiment B lacking the trait variability corridor, the distribution is shifted towards the lower *SLAs*. For experiment C lacking the *SLA*-*LL* trade-off, the distribution is shifted strongly towards the higher *SLAs*.

Fig. 4: Trait distributions simulated at each grid cell of the entire Amazon region. Shown are the expectation values *E* and scale parameters σ of the fitted log-normal distributions (cf. Fig. 2) under the settings of experiment A. Left panels (a, c, e): Expectation values *E*. Right panels (b, d, f): Scale parameter σ (right panels). *E* indicates the most probable trait value and σ is a measure of trait variability of the log normal probability density functions of specific leaf area (*SLA*, a-b), leaf longevity (*LL*, c-d), and wood density (*WD*, e-f) distributions, respectively. a.) Trees with lower *SLAs* establish in the North-Western wetter part of the Amazon region, whereas those with higher *SLAs* establish in the South-Eastern drier part of the Amazon region. Circles in (a) indicate locations L1-L4 with sufficient TRY data to compare empirical to simulated *SLA* distributions (cf. Fig.2). Coordinates of sites (longitude, latitude): L1 (-60.75, -14.75); L2 (-60.25, -2.75); L3 (-76.25, -0.75); L4 (-69.25, -12.75). b.) The σ of the *SLA* distribution is higher in the drier parts of the Amazon and lower in the wetter parts of the Amazon. c.) The *E* of *LL* is higher in wetter parts of the region. d.) The σ of the *LL* distribution is higher in the drier and lower in the wetter areas. e.) *WD* shows high values in the northwestern and southern part, and low values in the central and eastern part of the Amazon. f.) As for *SLA* and *LL*, the σ of the *WD* distribution is higher (lower) in the drier (wetter) parts of the Amazon.

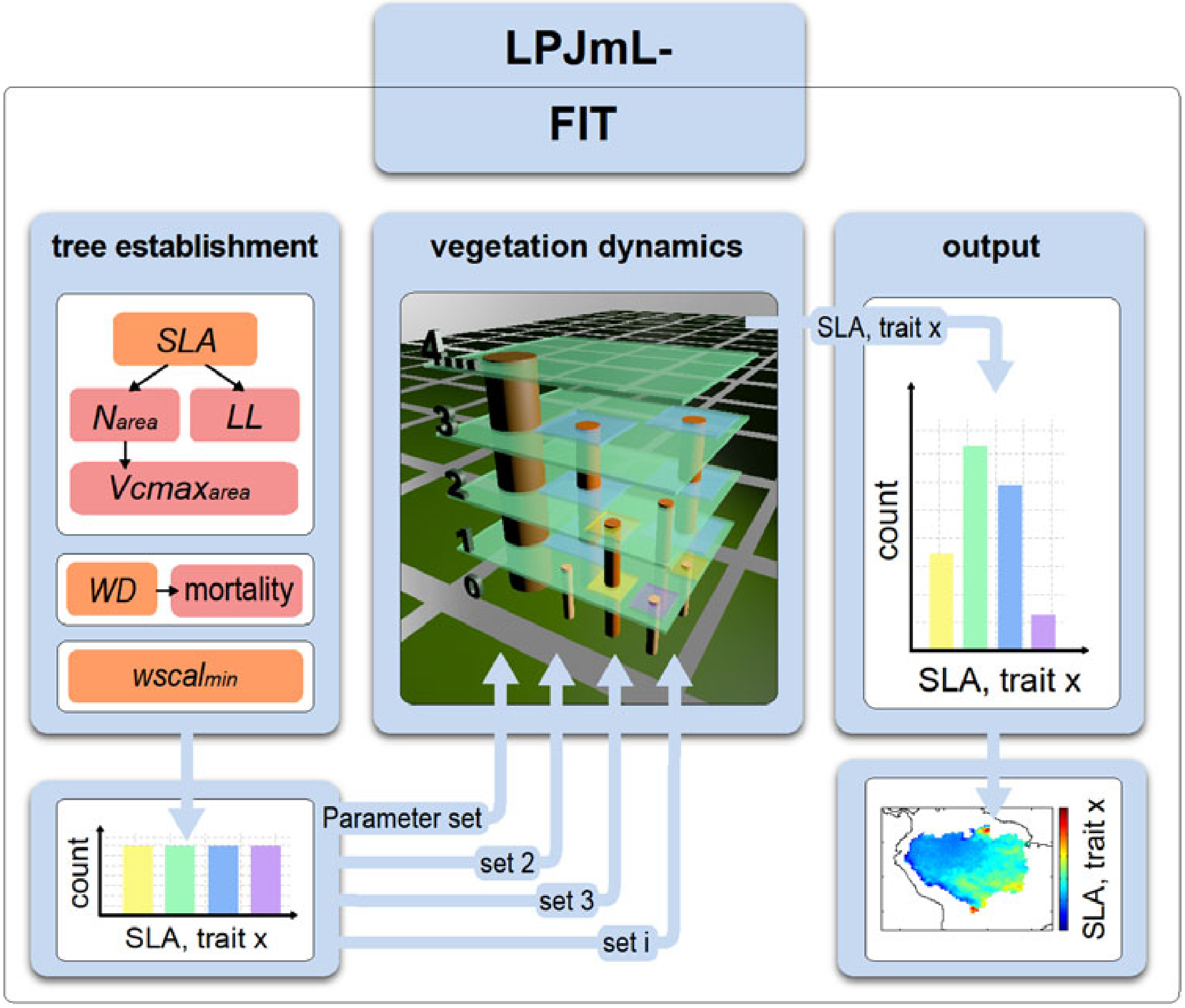
LPJmL-
FIT
tree establishment
SLA
Narea
LL
Vcmaxarea
WD
mortality
wscalmin
vegetation dynamics
4...
3
2
1
0
output
SLA, trait x
count
SLA, trait x
count
SLA, trait x
Parameter set
set 2
set 3
set i
SLA, trait x

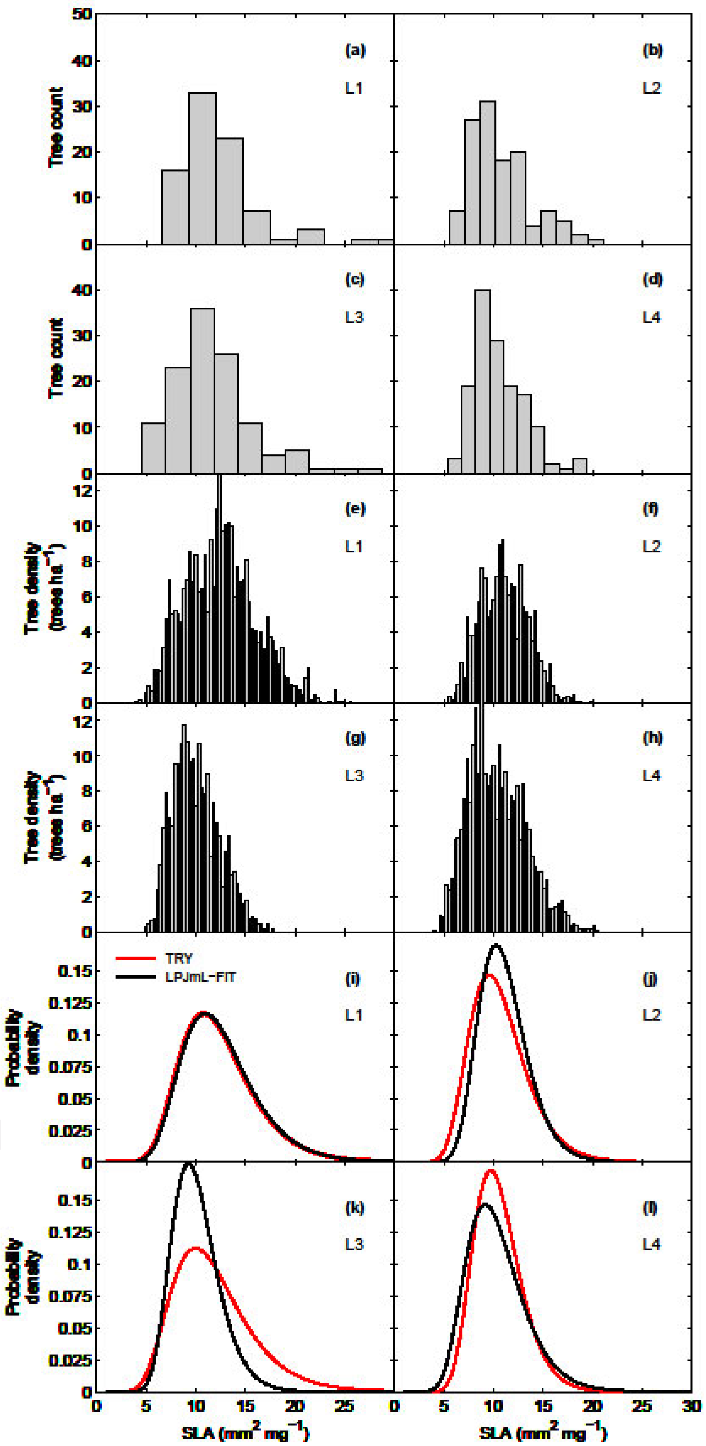
(a)
L1
(b)
L2
(c)
L3
(d)
L4
(e)
L1
(f)
L2
(g)
L3
(h)
L4
(i)
L1
(j)
L2
(k)
L3
(l)
L4
Tree count
Tree density (trees ha^{-1})
Probability density
TRY
LPJmL-FIT
SLA (mm^2 mg^{-1})

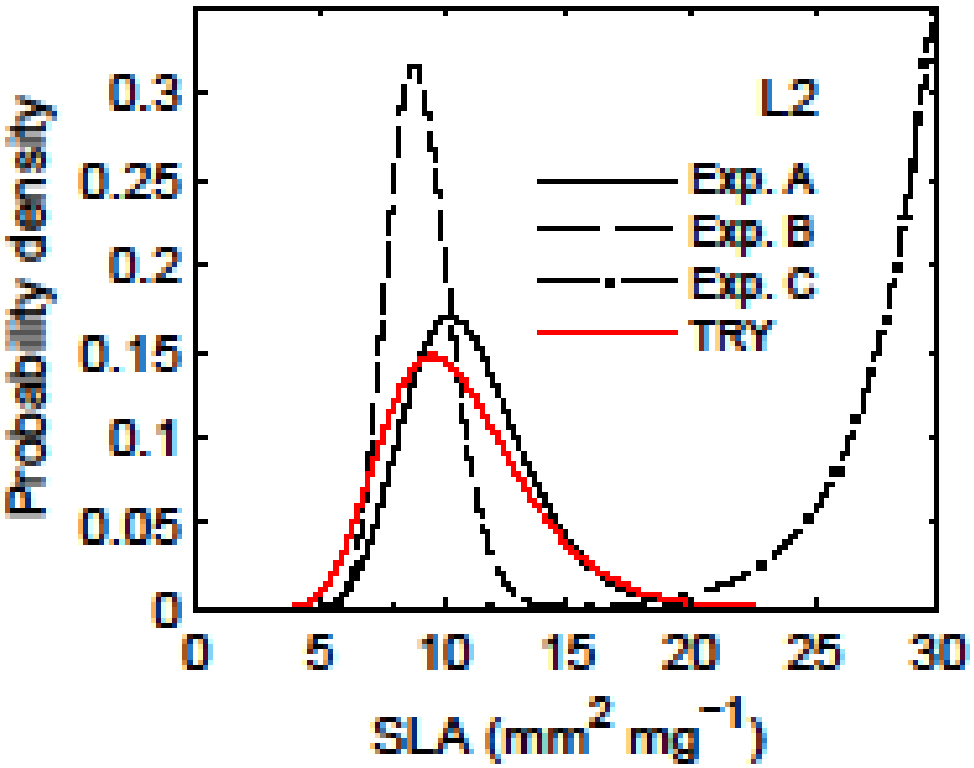
L2
Exp. A
Exp. B
Exp. C
TRY
Probability density
0.3
0.25
0.2
0.15
0.1
0.05
0
0
5
10
15
20
25
30
SLA (mm^2 mg^{-1})

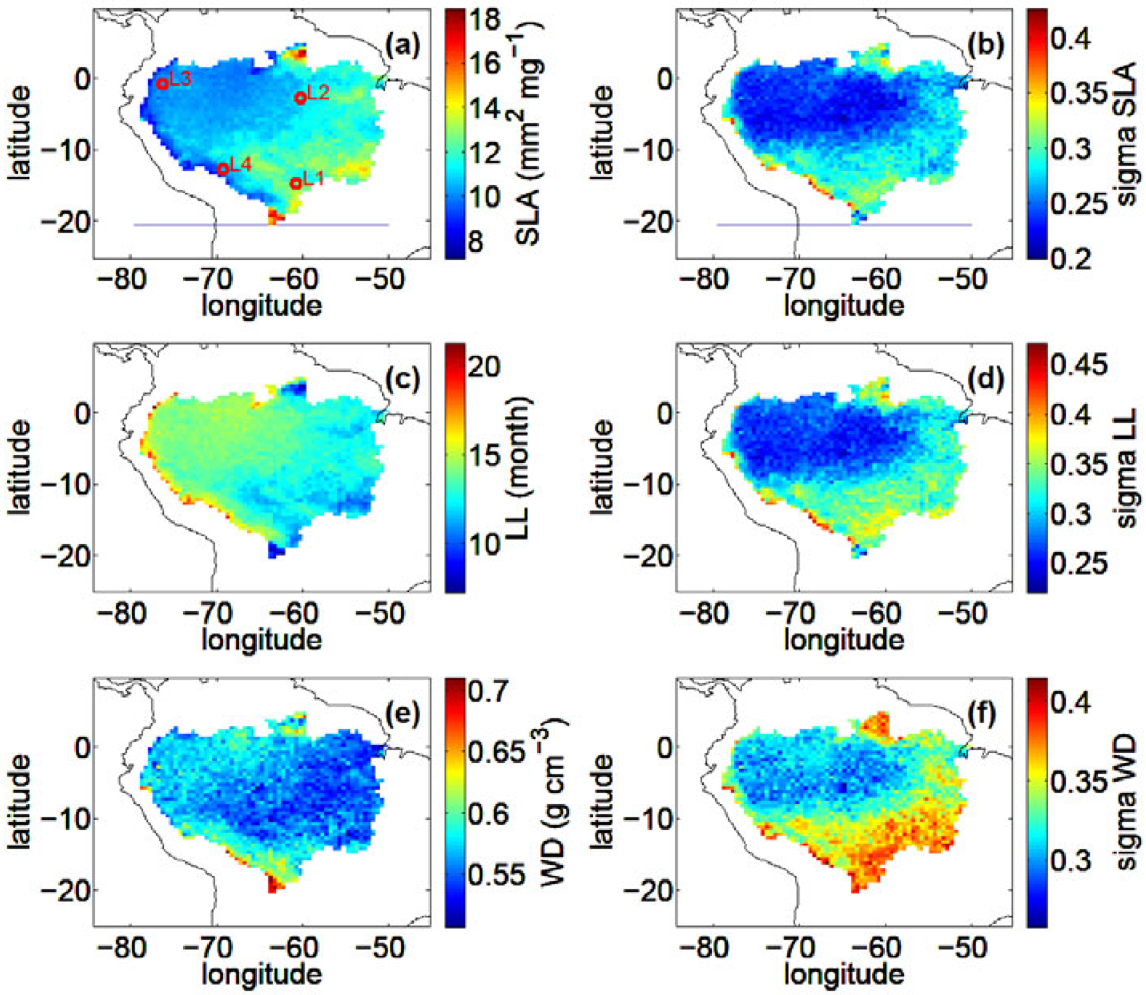
(a)
L3
L2
L4
L1
latitude
longitude
SLA (mm^2 mg^{-1})
(b)
sigma SLA
(c)
LL (month)
(d)
sigma LL
(e)
WD (g cm^{-3})
(f)
sigma WD